

Experimental Report template

Proposal title: Main role of heterogeneities on strain-induced crystallization of natural rubber thanks to in situ X rays scattering		Proposal number: 2015214
Beamline:	Date(s) of experiment: from: 26/07/16 to: 01/08/16	Date of report: 15/02/17
Shifts: 12	Local contact(s): Isabelle Morfin Nathalie Boudet	Date of submission: 15/02/17

Objective & expected results (less than 10 lines):

To complete the scarce data on SIC kinetic as a function of the average crosslink density, we propose a comparative study of SIC over a large strain rate domain, in rubbers with average EAC (Elastic Active Chains) densities in the range $[0.99 \times 10^{-4} \text{ mol.cm}^{-3} \text{ to } 1.76 \times 10^{-4} \text{ mol.cm}^{-3}]$. This selection is appropriate as it allows studying both under-vulcanized and over-vulcanized (compared to the density of the physical entanglements). Crystallization during in situ WAXS dynamic cycles is finally performed over the strain rate range $[7.2 \text{ s}^{-1} \text{ to } 1.44 \times 10^2 \text{ s}^{-1}]$ s in order to examine the influence of viscoelastic effects at high strain rates.

Results and the conclusions of the study (main part):

Effect of ν on the thermal stability of crystallites

Vulcanized rubbers are stretched and unstretched at $4.2 \times 10^{-3} \text{ s}^{-1}$ strain rate and room temperature, from the undeformed state up to $\lambda = 6$. As shown in figure 1, the stretching ratio at crystallization onset λ_c is around 4.3 for all samples, which is consistent with the literature. CI then increases and decreases during the loading and unloading steps respectively. The hysteretic shape of the curve is explained by the kinetics nature of the crystallization process while melting is characteristic of the equilibrium state. The melting stretching ratio λ_m increases from 2.5 to 3.3 when the average density ν increases. L_{200} is plotted as a function of CI in figure 1b. Only data measured during the unloading phase are reported, but similar trend is observed during the loading phase. L_{200} – and thus the average volume V of the crystallites increases with CI.

For a given CI, the crystallites size is always higher in the most weakly vulcanized sample. This larger crystallites size is associated with a lower melting stretching ratio λ_m , in other word a higher thermal stability.

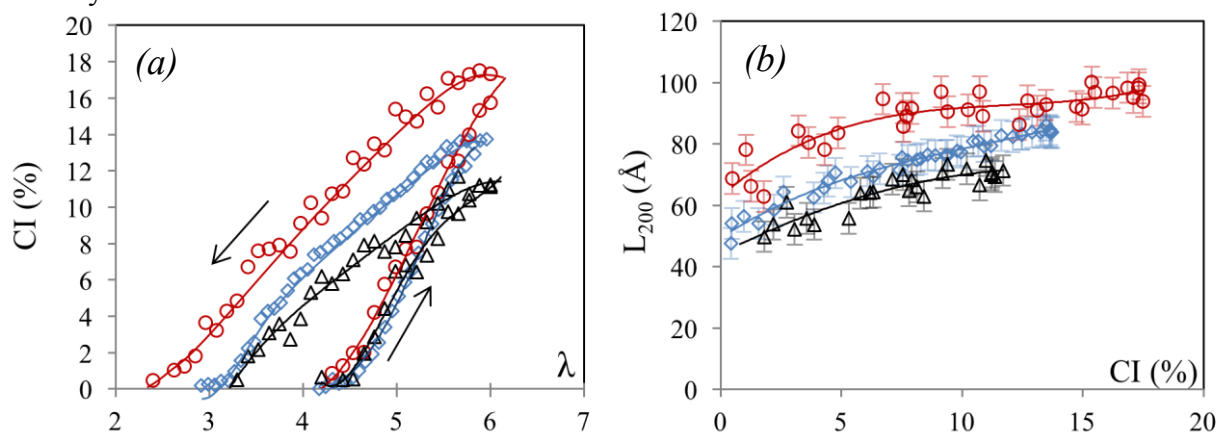


Figure 1. (a) CI during cyclic tests at room temperature and the strain rate $4.2 \times 10^{-3} \text{ s}^{-1}$ for NR_{0.8} (circle

symbols), NR_{1.2} (diamond symbols) and NR_{1.6} (triangle symbols). (b) L₂₀₀ versus CI during the unloading phase of cyclic test. Lines are guides for the eyes.

Melting is now studied at higher stretching ratio. Samples are stretched at room temperature and slow strain rate ($4.2 \times 10^{-3} \text{ s}^{-1}$) up to $\lambda = 6$. They are then relaxed during five minutes in order to ensure a stabilization of the SIC process. Only weak variation of the crystalline structure is observed during this phase whatever the material. The samples are finally heated from room temperature up to the temperature of total melting of crystallites T_m . Figure 2 and 3 present CI and L₂₀₀ as a function of the time during the stretching and relaxation steps, and as a function of the temperature during the heating step. Melting of crystallites in stretched sample (at $\lambda = 6$) is associated with a decrease of L₂₀₀, which is similar to the one observed during unloading at room temperature (figure 1). In particular, the sizes of the last crystallites that melt during heating at $\lambda = 6$ or during unloading at room temperature are roughly the same. The melting curves CI(T) seem to converge and the temperature of total melting of crystallites is around 110°C for NR_{1.6} and NR_{1.2} and 120°C for NR_{0.8}.

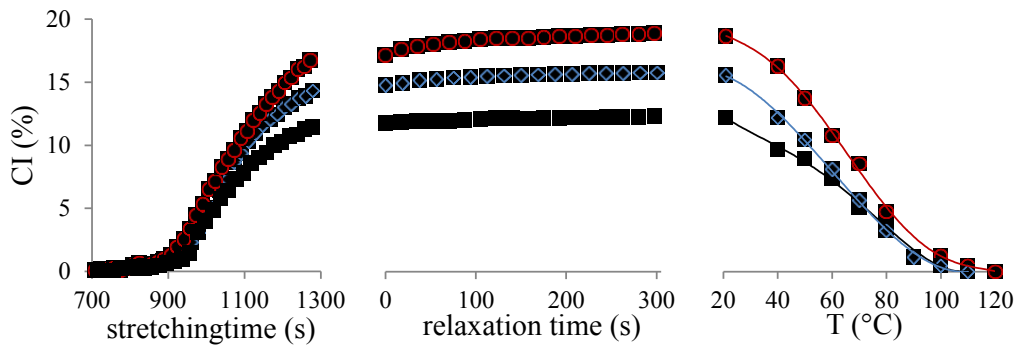


Figure 2. CI during stretching, relaxation and melting in the deformed state $\lambda=6$ for NRS_{0.8} (circle symbols), NRS_{1.2} (diamond symbols) and NRS_{1.6} (triangle symbols) samples.

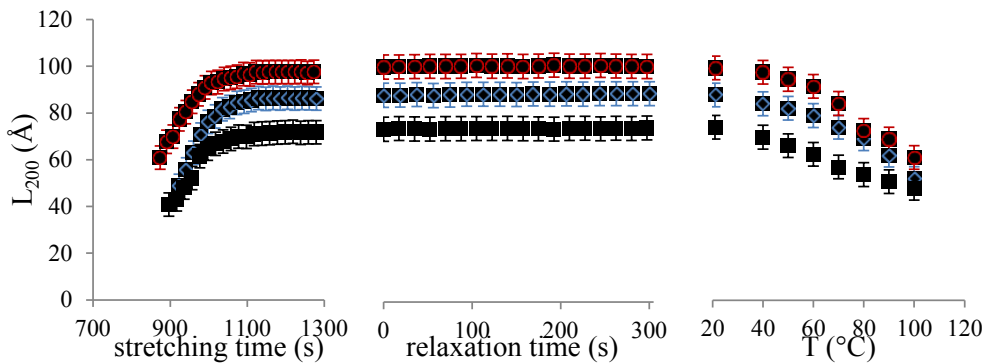


Figure 3. L₂₀₀ during stretching, relaxation and melting in the deformed state $\lambda=6$ for NRS_{0.8} (circle symbols), NRS_{1.2} (diamond symbols) and NRS_{1.6} (triangle symbols) samples.

Classical SIC theories predict that the melting temperature should increase when polymer chains are oriented by a macroscopic stretching of the sample. Numerous experimental works, as well as the present work, also show such a trend.

SIC kinetics of vulcanized natural rubbers

In industrial applications (e.g. pneumatic tires), rubber is generally submitted to complex solicitations, such as cyclic ones at high frequency. With the aim of applying more realistic mechanical conditions than a simple monotonic stretch, and also to directly observe SIC through in situ WAXS, cyclic tests are carried out thanks to the experimental device described in section 2.4. NR_{0.8}, NR_{1.2} and NR_{1.6} samples are first quickly pre-stretched at $\lambda_a = 3.9$ and let relaxed in the deformed state during five minutes. Samples are then dynamically deformed around λ_a with an amplitude $\Delta\lambda = \lambda_{\max} - \lambda_{\min} = 1.8$. The frequency varies from 2 Hz to 40 Hz, and the corresponding strain rates extend from 7.2 s^{-1} to 144 s^{-1} . The important point here is that for fixed pre-stretched and dynamic amplitude, the dynamic cycle evolves totally (NR_{0.8} and NR_{1.2}) or partially (NR_{1.6}) above the melting stretching ratio λ_m at room temperature (as schematized in figure 7), if one

assumes that λ_m is independent of the strain rate of the cycle.

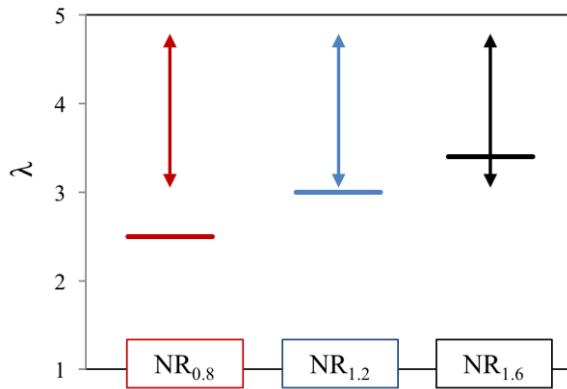


Figure 4. λ domain of the dynamic stretching ratio (vertical arrows) and λ_m at room temperature deduced from figure 1 (horizontal lines).

The evolution of the crystalline cycles during dynamic tests for NR_{1.2} and NR_{1.6} samples is presented in figure 5. Slow strain rate cycles are added for comparison. Because λ_{min} is below or close to λ_m (for NR_{1.6} and NR_{1.2} respectively) at room temperature (deduced from the unloading phase of the slow strain rate cycle at room temperature), CI at λ_{min} is expected to be equal or close to zero, whatever the frequency tested, as found experimentally. For both materials, CI increases from λ_{min} to λ_{max} and decreases from λ_{max} to λ_{min} . Thus, some SIC is found for all the frequencies, for both NR1.2 and NR1.6. Looking back at the results presented in figure 6, at 2Hz, which corresponds to a maximum strain rate of 7.2s⁻¹ (maximum as the strain cycle is a sinewave), λ_c of NR1.2 becomes very close to λ_{max} ; unfortunately we did not performed measurements for NR1.6, but we can assume that this is also the case for NR1.6. This should lead to a very weak SIC whatever the tested frequencies; nevertheless, the measured SIC stays significant at 2Hz and above, which might be explained by viscoelastic effects at these large frequencies, as discussed further with NR0.8 for which these effects are much more obvious. Here, with NR1.2 and NR1.6, they do not need to be important, as a small reduction of λ_c at 2Hz (maybe due to some trapping of entanglement at high strain rate) is sufficient to explain the obtained results. Indeed, even if the onset of cristallisation for the first loading phase is only slightly below λ_{max} at 2Hz, the protocole of our experiment explains that SIC can be also measured at 15Hz : as found in a previous work³², the chains of the crystallites which have molten during unloading seem to keep the memory of their previous alignment, this facilitates the crystallites re-nucleation during the following loading step and therefore leads to a decrease of the onset of cristallisation down to λ_m . One observe however that SIC becomes weaker when the frequency increases above 2Hz, because of self-heating effect which has also to be taken into account: it is known to leads to an increase of the stretching ratio for both nucleation and melting of the different crystallites populations.

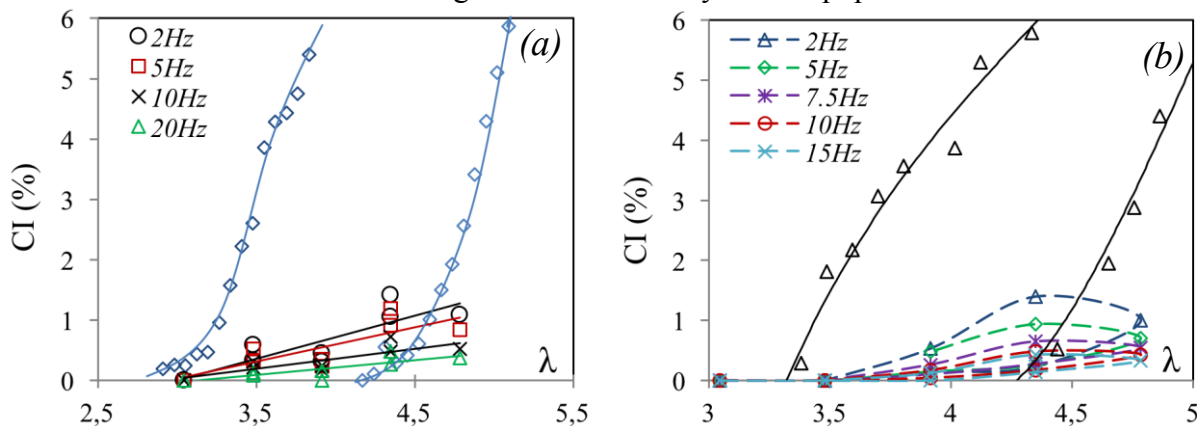


Figure 5. CI versus stretching ratio for NR_{1.2} (a) and NR_{1.6} (b) samples during dynamic test at various frequencies. CI curves at slow strain rate and room temperature are re-called (same data of figure 1).

Figure 6 now displays the evolution of CI of NR_{0.8} during dynamic cycles. At 2Hz, a residual CI is measured at λ_{min} . This is expected because (i) λ_{min} is above λ_m at room temperature and (ii) self-heating at this

frequency is negligible. However, CI at λ_{\min} becomes null between 10Hz and 20Hz. For these frequencies, the surface temperature is found equal to 29 and 31°C respectively, due to a self-heating. At these temperatures, λ_m estimated is found equal to 3.2 and 3.3 respectively, i.e. just above λ_{\min} . Thus, assuming the equivalence between self-heating and heating brought by an external source, and also that λ_m is only temperature but not strain rate dependent, CI disappearance at λ_{\min} for frequency above 10Hz is well explained. Same reasoning applied to synthetic filled NR tested in same conditions led to similar conclusions.

Contrarily to the the CI curve of NR_{1,2} and NR_{1,6}, the CI curves of NR_{0,8} exhibit large hysteretic shape at 2Hz. The CI measured at the beginning of the unloading (11.5%) is much higher than the maximum value that would be expected if the cycle was carried out at slow strain rate: 4.5% is the value measured at $\lambda = \lambda_{\max}$ during the loading phase of the cyclic test at slow strain rate. During unloading, CI then immediately decreases down to 1%. This acceleration of melting compared to the unloading curve at slow strain rate might be due to the fact that the amorphous chains surrounding the crystallites do not have sufficient time to relax and to make the crystalline phase stable. Note that an increase of the frequency from 2 Hz to 5 Hz does not change the cycle shape. These results confirm the larger ability of this material to crystallize at high strain rates, compared to more vulcanized sample. They are in agreement with the result of figure 6. Indeed, in the same range of strain rates (from 1 s⁻¹ to 10 s⁻¹), it was found the lowest values of λ_c for NR_{0,8}. At 2Hz, the size of the crystallites at the maximum of CI has been astonishingly found around 110 Å, i.e. much above the largest crystallite average size found at low strain rate (cf. Figure 1b). Thus, at 2Hz, by comparison with slow strain rate cycle, the crystallinity might be the results of a larger amount of large crystallites. In addition, it is noteworthy that (i) the largest CI is not found at the maximum stretching ratio, but at a stretching ratio slightly lower, and (ii) the CI increase is very large between these two stretching ratios. This indicates complex viscoelastic effects probably related to the dynamics of the entanglements in the material, and which, for a part of them, are not trapped by the chemical crosslinks, as it is mainly the case in more crosslinked sample (for instance NR_{1,2}). As previously said, we think that these entanglements might act, at large strain rate, as supplementary crosslinks enabling an easier nucleation of the crystallites, and might also have sufficient mobility (as they are not completely trapped by the chemical crosslinks) to enable the growth of larger crystallites from the nuclei.

As expected, at 10 Hz and above, self-heating and the increase of the nucleation time, which turns out to be too large compared to the experimental time, probably become the predominant effects. It should be recalled that this frequency corresponds to an experimental time which in the range of the characteristic times for SIC recently measured by different authors^{21,31,38,41}. Its leads to a decrease of CI with the frequency, like it was also observed for the more vulcanized rubbers NR_{1,2} and NR_{1,6}.

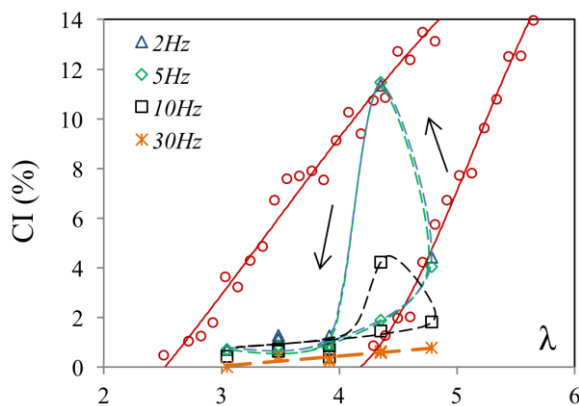


Figure 6. CI versus stretching ratio for NR_{0,8} sample during dynamic test at various frequencies. CI curves at slow strain rate and room temperature are re-called (cf. figure 1).

Conclusion

Strain Induced Crystallization (SIC) of Natural Rubbers (NR) with different network chain densities (ν) is studied. For the weakly vulcanized rubber, the melting stretching ratio λ_m at room temperature is the lowest. This is correlated with larger crystallites in this material measured by in situ WAXS, suggesting their higher thermal stability. SIC kinetics is then studied via stretching at various strain rates (from $5.6 \times 10^{-5} \text{ s}^{-1}$ up to $2.8 \times 10^1 \text{ s}^{-1}$). For the slowest strain rates, SIC onset (λ_c) is clearly the lowest in weakly vulcanized rubber.

By increasing the strain rate, λ_c of the different materials increase and converge. For the highest strain rates, λ_c values still increase but less rapidly for the weakly vulcanized sample. This complex dependence on the elastically active chains (EAC) density of SIC has been confirmed by in situ WAXS during dynamic experiments and interpreted as a consequence of both the polymer chain network topology and of the entanglements dynamics.

Justification and comments about the use of beam time (5 lines max.):

One day was necessary to install the tensile test machine and to set up the experiment. A complete study of every sample requires 1,5 to 2 hours of measurement. The 12 shifts were necessary to complete our experimental program.

Publication(s):

Writing in progress

International Conferences :

- 1- 16th European Polymer Federation (EPF), Lyon , 2-7/07/2017
- 2- 10th European Conference on Constitutive Models for Rubbers (ECCMR), Munich, 28-31/08/2017